Inorg. Chem. **2006**, *45*, 304–314

Synthesis of a Large Amino-Phenolic Cage. Synthesis, Crystal Structures, and Acid–Base and Coordination Behavior toward Cations and Anions

Gianluca Ambrosi,[†] Paolo Dapporto,[‡] Mauro Formica,[†] Vieri Fusi,*[,†] Luca Giorgi,[†] Annalisa Guerri,[‡] Mauro Micheloni,*[,†] Paola Paoli,[‡] Roberto Pontellini,[†] and Patrizia Rossi[‡]

Institute of Chemical Sciences, University of Urbino, P.za Rinascimento 6, I-61029 Urbino, Italy, and Department of Energy Engineering "Sergio Stecco", University of Florence, Via S. Marta 3, I-50139 Florence, Italy

Received August 1, 2005

The synthesis and characterization of the new polyaza-phenolic-macrobicycle 32-hydroxy-1,4,7,10,13,16,19,22-octaazatricyclo-[11.11.7.1^{26,30}]-diatriconta-26,28,$\Delta^{30,32}$-triene (**L**) are reported. **L** incorporates a 2,6-dimethyl-phenolic unit bridging two opposite amine functions of the [24]aneN$_8$ polyazamacrocyclic base to obtain a large cage. The basicity and binding properties of **L** toward Cu(II), Zn(II), and Cl$^-$ were determined by means of potentiometric measurements in aqueous solution (298.1 ± 0.1 K, I = 0.15 mol dm^{-3}). **L** can add up to six acidic protons, yielding the $H_5\mathbf{L}^{5+}$ species or the $H_6\mathbf{L}^{6+}$ species, depending on the ionic medium used. The molecular topology of **L** permits the formation of a highly positive three-dimensional cavity in the polyprotonated species that is able to host the chloride anion. This was detected both using potentiometric data, log K = 41.33 for the reaction $\mathbf{L} + 6H^+ + Cl^- = H_6\mathbf{L}Cl^{5+}$, and in ^{35}Cl NMR experiments that showed interactions also with the $H_5\mathbf{L}^{5+}$ and $H_4\mathbf{L}^{4+}$ species. The anion is probably hosted inside the three-dimensional cavity of **L**, and stabilized by H-bonding interactions with the ammonium groups, as depicted in the crystal structure of the $H_6\mathbf{L}^{6+}$ cation reported. **L** forms mono- and dinuclear complexes with all the metal ions investigated; the dinuclear species are the only existing species with an **L**:M(II) molar ratio of 1:2 at pH higher than 6. The phenolate oxygen atom coordinates the two metal ions in a bridged disposition, drawing them inside the macrobicyclic cavity. The two metals were found to be quite isolated by the medium, and were coordinated by all the amine groups of **L**, as shown by the crystal structure of the dinuclear $[Zn_2H_{-1}\mathbf{L}]^{3+}$ species. This species can bind guests such as hydroxide and phosphate anions. Studies of anion binding in aqueous solution using pyrochatecol violet as the sensing guest revealed that the $[Zn_2H_{-1}\mathbf{L}]^{3+}$ species is able to bind one phosphate at physiological pH.

Introduction

The properties of multifunctional molecules that are able to form supramolecular aggregates and are suitable to interact with guests having different charges and natures are challenging to study.[1,2] Polyamine ligands are an excellent starting point for molecular recognition studies, in that protonated species of polyazamacrocycles or their metal complexes are efficient receptors for different substrates.[3−6] In this field, one of the aims of synthetic design is to modify the polyamine skeleton by inserting one or more groups, thus producing dishomogeneity in the molecule. This approach changes the coordination parameters of the ligands, and allows the peculiar properties of the inserted group to be exploited.[7−12] From this standpoint, the phenol is an interest-

* To whom correspondence should be addressed. E-mail: vieri@uniurb.it.
[†] University of Urbino.
[‡] University of Florence.

(1) (a) Pedersen, C. J. *J. Am. Chem. Soc.* **1967**, *89*, 7017. (b) Lehn, J. M. *Pure Appl. Chem.* **1977**, *49*, 857. (c) Cram, D. J.; Cram, J. M. *Science* **1984**, *183*, 4127. (d) Lehn, J. M. *Angew. Chem., Int. Ed.* **1988**, *27*, 89.

(2) (a) Schneider, H. J.; Yatsimirsky, A. K. *Principles and Methods in Supramolecular Chemistry;* John Wiley & Sons: New York, 2000. (b) Steed, J. W.; Atwood, J. L. *Supramolecular Chemistry;* John Wiley & Sons: New York, 2000. (c) Voegtle, F. *Comprehensive Supramolecular Chemistry: Molecular Recognition*; Pergamon: New York, 1996; Vol. 2: Receptors for Molecular Guests. (d) Gokel, G. W. *Comprehensive Supramolecular Chemistry: Molecular Recognition;* Pergamon: New York, 1996; Vol. 1: Receptors for Cationic Guests

10.1021/ic051304v CCC: $33.50
Published on Web 11/08/2005

ing group, because its insertion strongly influences the coordinating and spectroscopic properties of the resulting molecule.[13,14] In fact, this aromatic moiety shows both photoactive and coordination properties; furthermore, this group can be employed as a building block for more-sensitive azo dyes.[15,16] The phenol units can behave as spectrophotometric probes for the interaction with a guest as well as in metal-ion coordination. Many of the biological active sites are formed by a transition dimetallic core in which the two metal ions cooperate with each other;[17−19] this makes the designing of new ligands that are able to form stable dinuclear complexes prone to interact with substrates interesting. In this light, the phenol is able to facilitate the assembling of two transition-metal ions in proximity to one another.

Chart 1

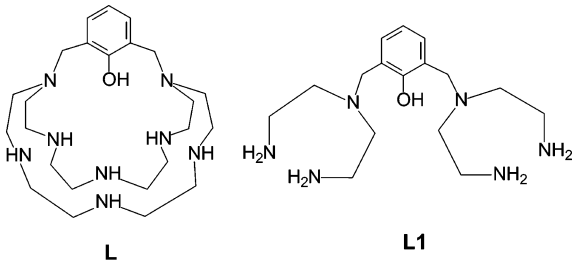

L **L1**

In the past few years, many molecular topologies, i.e., cyclic (macrocycles) and noncyclic molecules, based on amine and phenolic functions as building blocks of the molecular system have been synthesized.[13−15] In particular, we found that ligand **L1** (Chart 1) was able to assemble two transition-metal ions in proximity without saturating their coordination requirement.[20] This allowed for the use of the dimetallic core as a host for external species, such as nitric oxide and dioxygen, some of which are biologically important.[21,22] The aggregates hence formed always involved the two metal centers cooperating to bind the substrate, which was coordinated in a bridged disposition between the two metals.

By virtue of the central role they play in both inorganic and biological processes, inorganic anions are often the substrates targeted for binding by a synthetic host. For instance, a large majority of substrates and cofactors engaged in biological processes are anions, and many of them are of inorganic nature; among these, phosphate and chloride are of special interest because of their ubiquitous presence in biological systems.

Taking into account the latter aspects and the binding properties of ligand **L1**, we synthesized the new molecule **L** (Chart 1) with the aim of extending the binding capability of the ligand. In fact, **L** has a molecular skeleton similar to that of **L1** but with a greater number of amine functions; moreover, it shows a macrocyclic topology, and can also be considered as being a large cage. In this case, it could be seen as the cage derived by bridging two opposite nitrogen atoms of the [24]aneN_8 aza-crown macrocyle with the 2,6-dimethylphenol unit. In this way, the possibility of assembling two transition metal ions close to each other, but lodged inside a macrobicyclic cavity, could be preserved; moreover, **L** should show a positively charged cavity at acidic pH values, and could be able to interact with simple anions that could be hosted inside it.

(3) (a) Zelewsky, A. *Stereochemistry of Coordination Compounds*; John Wiley & Sons: New York, 1996. (b) Constable, E. C. *Coordination Chemistry of Macrocyclic Compounds*; Oxford University Press: Oxford, 1999.
(4) (a) Hancock, R. D. *Metal Complexes in Aqueous Solution*; Modern Inorganic Chemistry; Plenum Press: New York, 1996. (b) Bradshaw, J.-S. *Aza-crown Macrocycles*; Wiley: New York, 1993. (c) Dietrich, P.; Viout, P.; Lehn, J.-M. *Macrocyclic Chemistry*; VCH: Weinheim, Germany, 1993.
(5) (a) Gokel, G. W. In *Crown Ethers and Cryptands;* Stoddart, J. F., Ed.; Monographs in Supramolecular Chemistry; The Royal Society of Chemistry: Cambridge, 1992. (b) Bianchi, A.; Bowman-James, K.; Garcia-España, E. *Supramolecular Chemistry of Anions*; Wiley-VCH: New York, 1997.
(6) (a) Formica, M.; Fusi, V.; Micheloni, M.; Pontellini, R.; Romani, P. *Coord. Chem. Rev.* **1999**, *184*, 347. (b) Kimura, E.; Gotoh, T.; Aoki, S.; Shiro, M. *Inorg. Chem.* **2002**, *41*, 3239. (c) Gokel, G. W.; Leevy, W. M.: Weber, M. E. *Chem. Rev.* **2004**, *104*, 2723.
(7) (a) Verdejo, B.; Aguilar, J.; Domenech, A.; Miranda, C.; Navarro, P.; Jimenez, H. R.; Soriano, C.; Garcia-Espana, E. *Chem. Commun*. **2005**, *24*, 3086. (b) Cangiotti, M.; Formica, M.; Fusi, V.; Giorgi, L.; Micheloni, M.; Ottaviani, M. F.; Sampaolesi, S. *Eur. J. Inorg. Chem.* **2004**, 2853.
(8) Fabbrizzi, L.; Foti, F.; Taglietti, A. *Org. Lett.* **2005**, *7*, 2603.
(9) (a) Gavrilova, A. L.; Bosnich, B. *Chem. Rev.* **2004**, *104*, 349. (b) Miranda, C.; Escarti, F.; Lamarque, L.; Yunta, M. J. R.; Navarro, P.; Garcia-España, E.; Jimeno, M. L. *J. Am. Chem. Soc.* **2004**, *126*, 823. (c) Lamarque, L.; Navarro, P.; Miranda, C.; Aran, V. J.; Ochoa, C.; Escarti, F.; Garcia-España, E.; Latorre, J.; Luis, S. V.; Miravet, J. F. *J. Am. Chem. Soc.* **2001**, *123*, 10560.
(10) Bencini, A.; Bianchi, A.; Fusi, V.; Giorgi, C.; Masotti, A.; Paoletti, P. *J. Org. Chem.* **2000**, *65*, 7686.
(11) (a) Fabbrizzi, L.; Leone, A.; Taglietti, A. *Angew. Chem.* **2001**, *40*, 3066. (b) Clares, M. P.; Aguilar, J.; Aucejo, R.; Lodeiro, C.; Albelda, M. T.; Pina, F.; Lima, J. C.; Parola, A. J.; Pina, J.; de Melo, J. S.; Soriano, C.; Garcia-Espana, E. *Inorg. Chem.* **2004**, *43*, 6114.
(12) (a) Mizukami, S.; Nagano, T.; Urano, Y.; Odani, A.; Kikuchi, K. *J. Am. Chem. Soc.* **2002**, *124*, 3920. (b) Xue, G.; Bradshaw, J. S.; Dalley, N. K.; Savage, P. B.; Krakowiak, K. E.; Izatt, R. M.; Prodi, L.; Montalti, M.; Zaccheroni, N. *Tetrahedron* **2001**, *57*, 7623.
(13) (a) Karlin, K. D.; Cruse, R. W.; Gultneh, Y.; Farooq, A.; Hayes, J. C.; Zubieta, J. *J. Am. Chem. Soc.* **1987**, *109*, 2668. (b) Berends, H. P.; Stephen, D. W. *Inorg. Chem.* **1987**, *26*, 749.
(14) (a) Dapporto, P.; Formica, M.; Fusi, V.; Micheloni, M.; Paoli, P.; Pontellini, R.; Romani, P.; Rossi, P. *Inorg. Chem.* **2000**, *39*, 4663. (b) Ambrosi, G.; Dapporto, P.; Formica, M.; Fusi, V.; Giorgi, L.; Micheloni, M.; Paoli, P.; Pontellini, R.; Rossi, P. *Chem.—Eur. J.* **2003**, *9*, 800.
(15) (a) Callan, J. F.; de Silva, A. P.; Magri, D. C. *Tetrahedron* **2005**, *61*, 8551. (b) Lee, D. H.; Im, J. H.; Son, S. U.; Chung, Y. K.; Hong, J.-I. *J. Am. Chem. Soc.* **2003**, *125*, 7752.
(16) (a) Bardazzi, E.; Ciampolini, M.; Fusi, V.; Micheloni, M.; Nardi, N.; Pontellini, R.; Romani, P. *J. Org. Chem.* **1999**, *64*, 1335. (b) Dapporto, P.; Formica, M.; Fusi, V.; Micheloni, M.; Paoli, P.; Pontellini, R.; Romani, P.; Rossi, P.; Valtancoli, B. *Eur. J. Inorg. Chem.* **2000**, 51. (c) Metivier, R.; Leray, I.; Valeur, B. *Chem. Commun.* **2003**, 996.
(17) (a) Lippard, S. J.; Berg, J. M. *Principles of Bioinorganic Chemistry*; University Science Books: Mill Valley, CA, 1994. (b) Reedijk, J., Ed. *Bioinorganic Catalysis*; Dekker: New York, 1993.
(18) (a) Karlin, K. D. *Science* **1993**, *261*, 701. (b) Wilcox, D. E. *Chem. Rev.* **1996**, *96*, 2435. (c) Hughes, M. N. *The Inorganic Chemistry of the Biological Processes*; Wiley: New York, 1981.
(19) (a) Agnus, Y. L. *Copper Coordination Chemistry: Biochemical and Inorganic Perspective*; Adenine Press: New York, 1983. (b) Bertini, I., Luchinat, C., Marek, W., Zeppezauer, M., Eds. *Zinc Enzymes*; Birkauser: Boston, 1986.
(20) (a) Dapporto, P.; Formica, M.; Fusi, V.; Micheloni, M.; Paoli, P.; Pontellini, R.; Rossi, P. *Inorg. Chem.* **2000**, *39*, 4663. (b) Dapporto, P.; Formica, M.; Fusi, V.; Giorgi, L.; Micheloni, M.; Paoli, P.; Pontellini, R.; Rossi, P. *Inorg. Chem.* **2001**, *40*, 6186.
(21) Ceccanti, N.; Formica, M.; Fusi, V.; Micheloni, M.; Pardini, R.; Pontellini, R.; Tinè, M. R. *Inorg. Chim. Acta* **2001**, *321*, 153.
(22) Cangiotti, M.; Cerasi, A.; Chiarantini, L.; Formica, M.; Fusi, V.; Giorgi, L.; Ottaviani, M. F. *Bioconjugate Chem.* **2003**, *14*, 1165.

Scheme 1. Synthesis of **L**

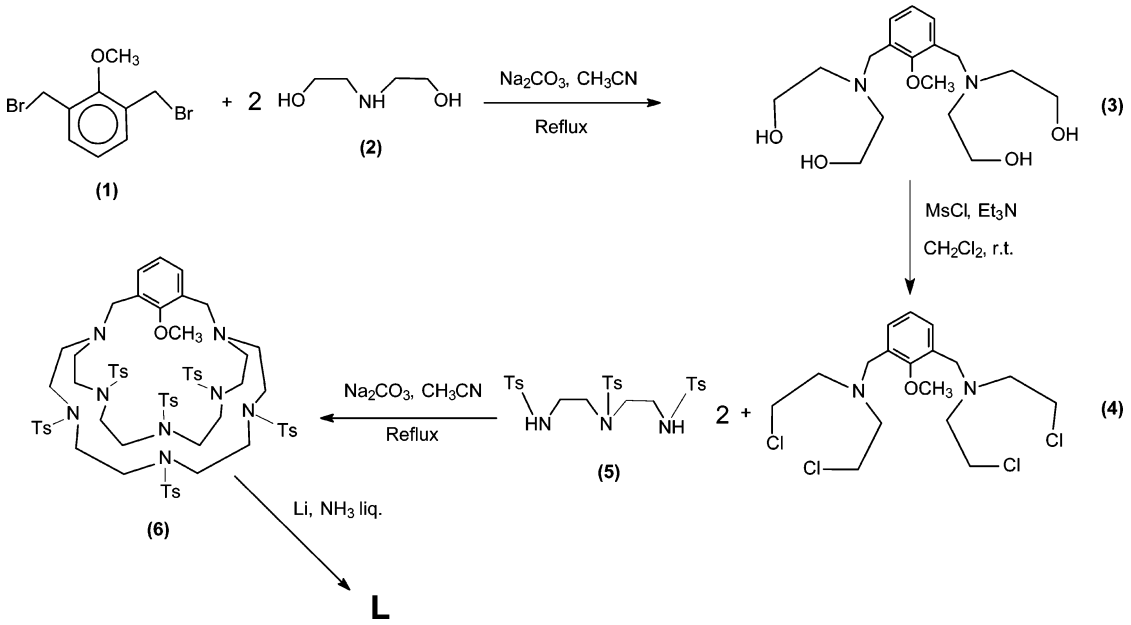

The synthesis and acid−base behavior of **L**, its coordination properties toward Cu(II) and Zn(II) transition-metal ions, and preliminary interaction studies with phosphate and chloride anions of both the free ligand and its Zn-dinuclear species in aqueous solution were investigated. The X-ray crystal structures of the protonated $H_6\mathbf{L}^{6+}$ and complexed $[Zn_2H_{-1}\mathbf{L}]^{3+}$ species of **L** were reported.

Experimental Section

General Methods. IR spectra were recorded on a Shimadzu FTIR-8300 spectrometer. Melting points were determined on a Büchi B 540 melting point apparatus, and are uncorrected. EI-MS spectra (70 eV) were recorded on a Fisons Trio 1000 spectrometer; ESI mass spectra were recorded on a ThermoQuest LCQ Duo LC/MS/MS spectrometer.

Synthesis. Ligand **L** was obtained following the synthetic procedure reported in Scheme 1. 2,6-Bis(bromomethyl)anisole (**1**)[23] and 1,4,7-tris(*p*-toluenesulfonyl)-1,4,7-triazapentane-1,5-diamine (**5**)[24] were prepared as previously described. All other chemicals were purchased, using the highest quality commercially available. The solvents were RP grade, unless otherwise indicated.

2,6-Bis{[bis(2-hydroxyethyl)amino]methyl}-1-methoxybenzene (3). A solution of diethanolamine (**2**) (10.5 g, 0.1 mol) in dry CH_3CN (200 cm^3) was added dropwise to a refluxing suspension of 2,6-bis(bromomethyl)anisole (**1**) (14.7 g, 0.05 mol) and K_2CO_3 (20.7 g, 0.3 mol) in dry CH_3CN (250 cm^3) under nitrogen. The reaction mixture was maintained under reflux for 4 h. After this time, it was filtered, and the solution was evaporated under reduced pressure. The crude product was dissolved in chloroform (150 cm^3), and the solution was washed with H_2O (3 × 50 cm^3). The organic layer was dried over Na_2SO_4, and the solvent was evaporated under reduced pressure, giving **3** as a white oil (15.1 g, 88%). MS *m*/*z* (EI): 342 $[M]^+$. ^1H NMR ($CDCl_3$, 25 °C): δ 7.25 (d, 2H), 7.06 (t, 1H), 3.82 (s, 3H), 3.64 (s, 4H), 3.54 (t, 8H), 3.31 (b, 4H), 2.61 (t, 8H). ^{13}C NMR ($CDCl_3$, 25 °C): δ 157.7, 132.3, 131.4, 124.4, 61.6, 59.4, 56.2, 54.6.

2,6-Bis{[bis(2-chloroethyl)-amino]methyl}-1-methoxybenzene (4). A solution of mesyl chloride (20.6 g, 0.18 mol) in dry CH_2Cl_2 (150 cm^3) was slowly added to a stirred solution of **3** (10.3 g, 0.03 mol) and triethylamine (24.3 g, 0.24 mol) in dry CH_2Cl_2 (150 cm^3) at 0 °C. The reaction mixture was stirred for 48 h at room temperature, and then evaporated under reduced pressure. The crude product was suspended in $CHCl_3$ (100 cm^3), and washed with 5% aqueous $NaHCO_3$ (4 × 50 cm^3) and brine (3 × 50 cm^3). The organic solution was dried over Na_2SO_4, and evaporated under reduced pressure. The yellow oil obtained was further purified by chromatography on neutral alumina ($CHCl_3$), affording **4** as a yellowish oil (7.6 g, 61%). MS *m*/*z* (EI): 367, $[M - CH_2Cl]^+$. ^1H NMR ($CDCl_3$, 25 °C): δ 7.39 (d, 2H), 7.11 (t, 1H), 3.78 (s, 4H), 3.76 (s, 3H), 3.53 (t, 8H), 2.93 (t, 8H). ^{13}C NMR ($CDCl_3$, 25 °C): δ 157.3, 131.8, 129.9, 124.2, 62.4, 56.3, 52.9, 42.0.

32-Methoxy-4,7,10,16,19,22-hexatosyl-1,4,7,10,13,16,19,22-octaazatricyclo-[11.11.7.1^{26,30}]-diatriconta-26,28,$\Delta^{30,32}$-triene (6). 4 (6.2 g, 0.015 mol) in 400 cm^3 of acetonitrile was added to a refluxing suspension of **5** (17.0 g, 0.030 mol) and K_2CO_3 (20.7 g, 0.15 mol) in 1 dm^3 of acetonitrile over a period of 4 h. The reaction mixture was maintained under reflux for 48 h, after which time the mixture was cooled to room temperature; the resulting suspension was evaporated under reduced pressure. The crude product was suspended in chloroform (150 cm^3) and filtered, and the organic layer was evaporated under reduced pressure, giving an orange solid. The crude product was purified by chromatography on activated II alumina, eluting with CH_2Cl_2, and **6** was obtained as a white solid (4.7 g, 22%). Anal. Calcd for $C_{67}H_{84}N_8O_{13}S_6$: C, 57.41; H, 6.04; N, 7.99. Found: C, 57.71; H, 6.20; N, 7.93. MS (ESI) (*m*/*z*): 1401.4 $(M + H^+)$. ^1H NMR ($CDCl_3$, 25 °C): δ 7.71 (m, 12H), 7.31 (m, 12H), 7.08 (d, 2H), 6.90 (t, 1H), 3.93 (b, 2H), 3.73 (b, 2H), 3.53 (s, 3H), 3.33 (b, 12H), 3.01 (d, 20H). 2.43 (s, 12H), 2.40 (s, 6H). ^{13}C NMR ($CDCl_3$, 25 °C): δ 158.7, 144.2, 143.7, 143.3, 136.6, 136.3, 134.6, 133.3, 133.0, 131.1, 130.1, 129.9, 129.8, 127.8, 127.5, 127.4, 127.2, 123.1, 61.6, 54.4, 53.8, 53.0, 51.6, 49.2, 48.7, 47.9, 21.6.

32-Hydroxy-1,4,7,10,13,16,19,22-octaazatricyclo-[11.11.7.1^{26,30}]-diatriconta-26,28,$\Delta^{30,32}$-triene (L). Ammonia (300 cm^3) was condensed on a suspension of **6**, (4.2 g, 3.0 mmol) in diethyl ether (30 cm^3) and methanol (1 cm^3) cooled to −70 °C. Little bits of

(23) Zazulak, W.; Chapoteau, E.; Czech, B.-P.; Kumar, A. *J. Org. Chem.* **1992**, *57*, 6720.
(24) Richman, J. E.; Atkins, T. J. *J. Am. Chem. Soc.* **1974**, *96*, 2268.

lithium were added to the mixture until the suspension turned blue. Thirty minutes after the suspension turned blue, NH_4Cl (12 g, 0.2 mol) was added. The white solid obtained after the evaporation of the solvents was treated with 3 mol dm^{-3} HCl (300 cm^3), and the resulting solution was washed with $CHCl_3$ (3 × 100 cm^3). The acidic solution was filtered, and then evaporated to dryness under reduced pressure. The resulting solid was dissolved in the minimum amount of water necessary, and the solution was made alkaline with concentrated NaOH solution. The liquid was extracted with $CHCl_3$ (6 × 50 cm^3). The organic layer was dried over Na_2SO_4, and vacuum-evaporated to obtain **L** as colorless oil (1.0 g, 74%). MS *m*/*z* (ESI): 463.4 ($[M + H]^+$). ^1H NMR ($CDCl_3$, 25°C): δ 6.83 (d, 2H), 6.53 (s, 1H), 3.42 (s, 4H), 3.27 (b, 1H), 2.69 (m, 24H), 2.43 (m, 8H). ^{13}C NMR ($CDCl_3$, 25°C): δ 155.8, 130.5, 123.7, 118.5, 55.6, 52.2, 49.0, 48.4, 45.6,.

L was further purified by dissolving it in ethanol (95%) and treating the solution with a 1:1 solution of ethanol (95%)/perchloric acid (70%) until there was complete precipitation of the dihydrated tetrahydroperchlorate salt **L**·$4HClO_4$·$2H_2O$ in almost quantitative yield as a white solid. ^1H NMR (D_2O, pH = 3): δ 7.31 (d, 2H), 7.06 (s, 1H), 3.92 (s, 4H), 3.28 (m, 24H), 3.02 (m, 8H). ^{13}C NMR (D_2O, pH = 3): δ 155.1, 135.7, 125.4, 124.3, 56.0, 51.0, 45.5, 45.3, 45.1. Anal. Calcd for **L**·$4HClO_4$·$2H_2O$, $C_{24}H_{54}Cl_4N_8O_{19}$: C, 32.01; H, 6.04; N, 12.44. Found: C, 32.16; H, 6.17; N, 12.36.

[H_6L]·6Cl·11H_2O (7). L (46.3 mg, 0.1 mmol) was dissolved in H_2O (3 cm^3), and the pH was adjusted to 2 with 0.1 M HCl; ethanol (10 cm^3) was added, and the solution obtained was kept at room temperature until colorless crystals suitable for X-ray analysis formed (62 mg, 70%). Anal. Calcd for [H_6**L**]·6Cl·$11H_2O$, $C_{24}H_{74}Cl_6N_8O_{12}$: C, 32.77; H, 8.48; N, 12.74. Found: C, 32.82; H, 8.63; N, 12.64.

[Zn_2(H_{-1}L)](ClO_4)$_3$ (8). A sample of $Zn(ClO_4)_2$·$6H_2O$ (37 mg, 0.1 mmol) in water (30 cm^3) was added to an aqueous solution (30 cm^3) containing **L**·$4HClO_4$·$2H_2O$ (45 mg, 0.05 mmol). The pH of the resulting solution was adjusted to 7.5 with 0.1 M NaOH, and saturated with solid $NaClO_4$; after a few minutes, **8** precipitated as a microcrystalline white solid (45 mg, 92%). Anal. Calcd for $C_{24}H_{46}Cl_3N_8O_{13}Zn_2$: C, 32.32; H, 5.20; N, 12.56. Found: C, 32.34; H, 5.14; N, 12.33. Crystal suitable for X-ray analysis was obtained by slow evaporation of a water solution containing **8**.

X-ray Crystallography. For compounds [H_6**L**]·6Cl·$11H_2O$ (**7**) and [Zn_2(H_{-1}**L**)](ClO_4)$_3$ (**8**) intensity data were collected on an Oxford Diffraction Xcalibur CCD area detector with graphite monochromated Mo Kα radiation (λ = 0.71070 Å). The temperature for the data collection of compound **7** was set at 200 K. Data collections were performed with the CrysAlis CCD program.[25] Two optimized sets of ω were collected with increments of 1° for each frame. Data reductions were carried out with the CrysAlis RED program.[26] In both cases, absorption correction was applied using the SADABS program.[27] Both structures were solved by direct methods (SIR97),[28] and refined by full matrix least squares on F^2 (SHELX97).[29]

Four chloride ions and nine oxygen atoms, the latter belonging to crystallization water molecules, were identified and successfully refined in the difference Fourier map of **7**. In addition, the interpretation of the four remaining isolated electron density peaks led us to take into account some degree of disorder in the crystal lattice. Each electron density peak was assigned to a couple of atoms: a chloride ion and an oxygen atom of a water molecule occupying the same position. The sum of the occupation factors of each pair was fixed at 1, but the individual values were refined and finally converged, resulting, as a whole, in two additional chloride ions and two oxygen atoms. Their thermal parameters were refined isotropically. All the other non-hydrogen atoms were set anisotropically. Hydrogen atoms were introduced in calculated positions, and refined isotropically with an overall temperature factor. For **8**, all the non-hydrogen atoms were refined anisotropically, whereas the hydrogen atoms were set in a calculated position and refined isotropically.

The graphical representations were carried out using the ORTEP3 program.[30] Bond lengths and angles were computed with the PARST97 program.[31] Crystallographic data and refinement parameters are reported in Table 1.

EMF Measurements. Equilibrium constants for protonation and complexation reactions with **L** were determined by pH-metric measurements (pH = $-\log[H^+]$) in 0.15 M NMe_4NO_3 at 298.1 ± 0.1 K, using the fully automatic equipment that has already been described;[20a] the EMF data were acquired with the PASAT computer program.[32] The combined glass electrode was calibrated as a hydrogen concentration probe by titrating known amounts of HNO_3 with CO_2-free NMe_4OH solutions and determining the equivalent point by Gran's method,[33] which gives the standard potential E^0 and the ionic product of water (pK_w = 13.78(1) at 298.1 K in 0.15 M NMe_4NO_3, $K_w = [H^+][OH^-]$). At least three potentiometric titrations were performed for each system in the pH range 2−11, using different molar ratios of Cl^-:**L** and M:**L** (M = Cu(II) and Zn(II)) ranging from 1:1 to 3:1. All titrations were treated as either single sets or separate entities for each system; no significant variations were found in the values of the determined constants. The HYPERQUAD computer program was used to process the potentiometric data.[34]

NMR Experiments. ^1H, ^{13}C, and ^{35}Cl NMR spectra were recorded on a Bruker Avance 200 instrument, operating at 200.13, 50.33, and 19.6 MHz, respectively, and equipped with a variable temperature controller. The temperature of the NMR probe was calibrated using 1,2-ethanediol as a calibration sample. For the spectra recorded in D_2O, the peak positions are reported with respect to HOD (4.75 ppm) for ^1H NMR spectra, whereas dioxane was used as reference standard in ^{13}C NMR spectra (δ = 67.4). For the spectra recorded in $CDCl_3$, the peak positions are reported with respect to TMS.

In ^{35}Cl NMR experiments, the spectra of the solutions were externally referenced at 298 K to 0.1 M NaCl.

UV−Vis Experiments. UV absorption spectra were recorded at 298 K on a Varian Cary-100 spectrophotometer equipped with a temperature control unit. The sensing solution for detecting the interaction with phosphate was prepared by mixing the dinuclear complex **8** and pyrocathecol violet (PCV) in a 10:1 molar ratio in

(25) *CrysAlis CCD*, version 1.171; Oxford Diffraction, Ltd.:Abingdon, U.K.; pre23_10 beta (release June 21, 2004, CrysAlis171.NET; compiled June 21, 2004, 12:00:08).
(26) *CrysAlis RED*, version 1.171; Oxford Diffraction, Ltd.: Abingdon, U.K.; pre23_10 beta (release June 21, 2004, CrysAlis171. NET; compiled June 21, 2004, 12:00:08).
(27) Sheldrick, G. M. *SADABS*; University of Göttingen: Göttingen, Germany, 1996.
(28) Altomare, A.; Cascarano, G. L.; Giacovazzo, C.; Guagliardi, A.; Burla, M. C.; Polidori, G.; Camalli, M. *J. Appl. Crystallogr.* **1999**, *32*, 115.
(29) Sheldrick, G. M. *SHELX 97*; University of Göttingen: Göttingen, Germany, 1997.
(30) Farrugia, L. J. *J. Appl. Crystallogr*. **1997**, *30*, 565.
(31) Nardelli, M. *Comput. Chem*. **1983**, *7*, 95.
(32) Fontanelli, M.; Micheloni, M. I Spanish-Italian Congress on Thermodynamics of Metal Complexes, Peñiscola, Spain, June 3−6, 1990; University of Valencia, Spain; 41.
(33) (a) Gran, G. *Analyst* **1952**, *77*, 661. (b) Rossotti, F. J.; Rossotti, H. *J. Chem. Educ.* **1965**, *42*, 375.
(34) Gans, P.; Sabatini, A.; Vacca, A. *Talanta* **1996**, *43*, 1739.

Table 1. Crystallographic and Refinement Data for Compounds **7** and **8**

	7	**8**
empirical formula	$[C_{24}H_{52}N_8O]\cdot 6Cl\cdot 11H_2O$	$[C_{24}H_{45}N_8OZn_2]\cdot 3(ClO_4)$
formula weight	879.61	890.8
T (K)	200	298
wavelength (Å)	0.71070	0.71070
cryst syst, space group	monoclinic, $P2_1/a$	orthorhombic, *Pbcn*
a (Å)	18.483(3)	15.252(2)
b (Å)	13.674(2)	15.419(3)
c (Å)	19.648(2)	14.605(3)
α (deg)	90	90
β (deg)	117.65(1)	90
γ (deg)	90	90
V (Å^3)	4399(1)	3435(1)
Z, calcd density (g/cm^3)	4, 1.328	4, 1.723
abs coeff (mm^{-1})	0.449	1.705
F(000)	1888	1840
cryst size (mm^3)	0.4 × 0.3 × 0.2	0.3 × 0.2 × 0.2
θ range for data collection (deg)	4.02−0.43	4.01−32.54
limiting indices	$-20 \le h \le 16$, $-18 \le k \le 18$, $-27 \le l \le 22$	$-20 \le h \le 17$, $-22 \le k \le 20$, $-20 \le l \le 19$
no. of reflections collected	16691	17138
refinement method	full-matrix least-squares on F^2	full-matrix least-squares on F^2
data/restraints/params	3038/0/448	2438/0/228
GOF on F^2	1.014	1.123
final R indices [$I > 2\sigma(I)$]	R1 = 0.0886, wR2 = 0.1836	R1 = 0.0896, wR2 = 0.1093
R indices (all data)	R1 = 0.2419, wR2 = 0.2548	R1 = 0.2095, wR2 = 0.1415

an aqueous solution of 10 mM HEPES buffer at pH = 7.0; the final concentration of **8** was 4.0 × 10^{-4} M. Buffered HEPES solutions containing inorganic (Cl^-, Br^-, NO_3^-, SO_4^{2-}, PO_4^{3-}) or organic (4-nitrophenylphosphate and bis(4-nitrophenyl)phosphate) anions up to 5 equiv with respect to the complex **8** were added to the solution.

Results and Discussion

Synthesis. The synthetic pathway used to obtain the ligand **L** is depicted in Scheme 1. The reaction used allows the synthesis of the tetra-alcohol **3** obtained by reacting 2,6-bis-(bromomethyl)-anisole **1** with 2 equiv of diethanolamine **2**. Compound **3** was reacted with methanesulfonyl-chloride (MsCl) to activate it for cyclization. This reaction leads to the tetrachloride **4** instead of the methanesulfonyl derivative predicted, because of the presence of the amine group in the β-position with respect to the hydroxyl functions that support the elimination of the MsO^-, giving rise to the formation of the more stable chloro derivative. The synthesis of tosylated macrocycle **6**, a modification of the Richman−Atkins method, involves the cyclization of 2 equivof the tritosylated polyamines **5** with 1 equiv of the tetrachloride derivative **4** in the presence of the base K_2CO_3. The final compound was obtained via a 2+1 cyclization scheme that gives, as the main product of the cyclization, **6** in 22% yield. This cyclization differs from that previously used to obtain similar ligands that yielded a different isomer of cyclization as the main product.[35] The cleavage reaction of the *p*-toluenesulfonyl groups of **6** was carried out with lithium in liquid ammonia. The reducing conditions of the treatment also produced the demethylation reaction of the ethereal methyl group of the anisole, obtaining ligand **L** after the described workup. The product can be further purified as hydrochloride or perchlorate salt.

(35) Ambrosi, G.; Dapporto, P.; Formica, M.; Fusi, V.; Giorgi, L.; Guerri, A.; Micheloni, M.; Paoli, P.; Pontellini, R.; Rossi, P. *J. Chem. Soc., Dalton Trans.* **2004**, *21*, 3468.

Description of the Structures. $[H_6L]\cdot 6Cl\cdot 11H_2O$ (7). The crystal lattice contains an independent hexaprotonated ligand $[H_6L]^{6+}$, 6 chloride ions, and 11 water molecules (see Experimental Section). The symmetric distribution of the positive charge residing on the secondary nitrogen atoms is corroborated also by the nearly identical 1−4 Å distances separating the latter (mean = 3.2 Å), which correspond to almost comparable N−C−C−N dihedral angles (>67°). As a result of electrostatic repulsion, the macrocyclic cavity is quite large. Its 24 atoms are equally distributed in three mean planes (Figure 1) that are almost parallel (15° is the mean angle formed between the planes) and equidistant to each other (the distance between their geometric centers is ca. 1.9 Å). The phenol mean plane forms an angle of 23.6(1)° with the closest plane comprising N(1) and N(5). The latter are about 5.7 Å from each other, a distance comparable with that observed in the corresponding metal complex **8** (5.9 Å).

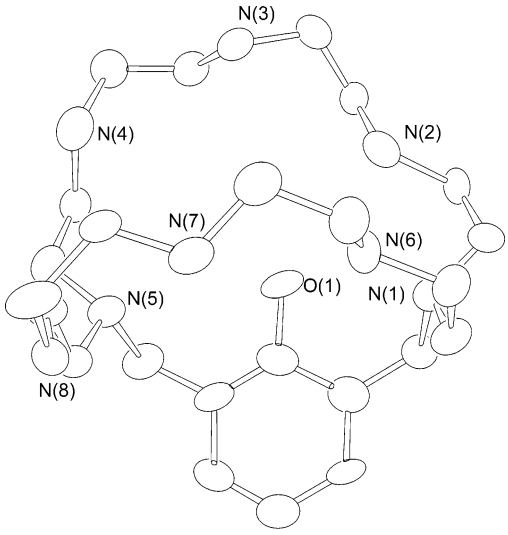

Figure 1. ORTEP view of the hexaprotonated species $[H_6L]^{6+}$. Thermal ellipsoids are drawn at a 30% level of probability.

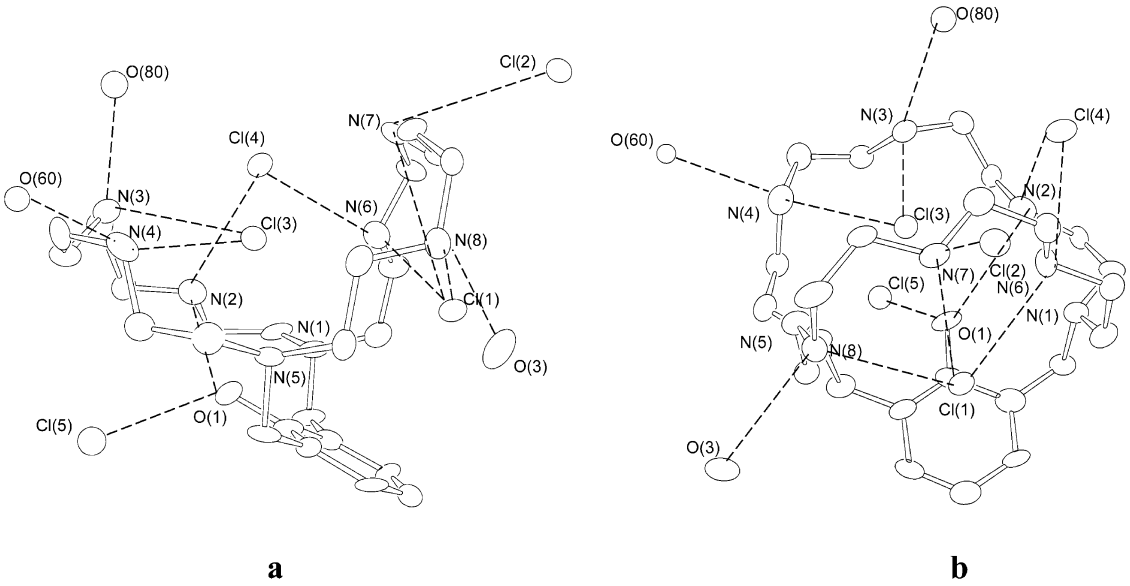

Figure 2. Side (a) and front (b) views of $[H_6\mathbf{L}]^{6+}$ species, highlighting the intermolecular contacts. Thermal ellipsoids are drawn at a 30% level of probability.

The four atoms N(2), N(4), N(6), and N(8) belonging to the plane located in the middle of the cavity are at the vertexes of an irregular square and about 5 Å from each other. Finally, the distance separating the facing N(3) and N(7) atoms, which reside at the top of the nitrogen cage, is 6.7 Å.

The high positive charge, together with the large number of H-bond donors, makes $[H_6\mathbf{L}]^{6+}$ able to interact with many chloride ions as well as water molecules. Within the thick net of interactions involving the hexaprotonated ligand, two main H-bond interactions (distinguished on the basis of geometrical criteria)[36] were identified and discussed for each of the six NH_2^+ groups. The macrocycle acts as a receptor for the ion Cl(3) ion, which is set into its cavity almost equidistant between N(3) and N(4) (the N···Cl distances are 3.136(7) and 3.291(7) Å, respectively), and acts as a bridging unit between them (Figure 2a). These two nitrogen atoms further interact via N−H···O bonds with the water O(80) (N···O 2.72(1) Å) and O(60) (N···O 2.87(2) Å) atoms, which are kept quite close to the molecular surface (see Figure 2b; the oxygen atoms share their positions with as many chloride ions). A net of H-bonds involving N(6), N(7), and N(8) keeps Cl(1) just outside the cavity (Figure 2a), with a mean N···Cl distance of 3.12 Å. The water O(3) atom acts as an H-bond acceptor with respect to the NH_2^+ group labeled N(8) (N···O 3.04(1) Å). In addition, N(6) and N(7) work as H-bond donors with respect to the Cl(4) and Cl(2) ions, respectively (N(6)···Cl(4) 3.148(8) Å and N(7)···Cl(2) 3.049-(5) Å). Whereas Cl(2) is definitely outside the macrobicycle (Figure 2a), Cl(4) resides at the top of the cation quite close to the molecular surface (Figure 2b), and also interacts with the N(2) (N···Cl 3.143(6) Å). N(2) further interacts with the phenol O(1) atom (N···O 3.08(1) Å), which is also an H-bond donor with respect to the Cl(5) ion (O(1)···Cl(5) 2.961(7) Å).

Finally, there are many interactions involving the chloride ions and the water oxygen atoms.

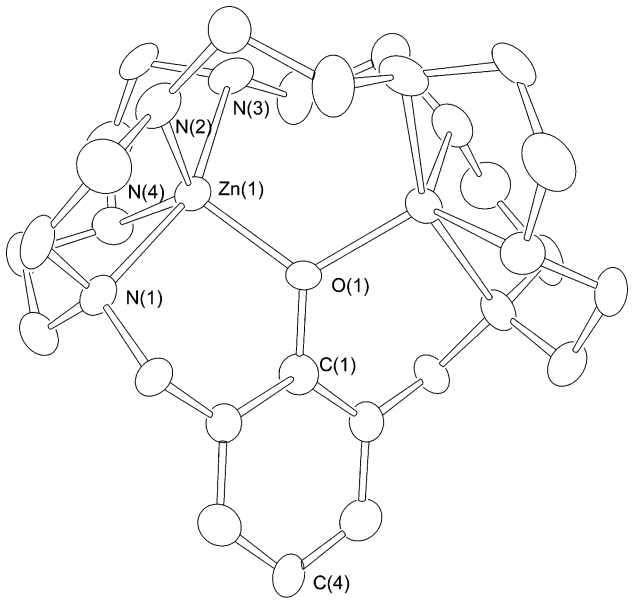

Figure 3. ORTEP view of the complex cation $[Zn_2(H_{-1}\mathbf{L})]^{3+}$. Thermal ellipsoids are drawn at a 30% level of probability.

$[Zn_2(H_{-1}L)](ClO_4)_3$ (8). The asymmetric unit of **8** contains half of the dinuclear complex and one and a half perchlorate anions. A 2-fold axis passing through atoms O(1), C(1), and C(4) of the phenolate moiety relates the two halves (see Figure 3). The two Zn(II) ions are 3.331(1) Å apart, and arranged on opposite sides with respect to the aromatic ring (Figure 3). Each metal cation is pentacoordinated by the phenol O(1) atom and four nitrogen atoms provided by the polyaza macrobicycle. Bond lengths concerning the coordination sphere are in the usual range (Table 2). The geometry (square pyramidal (sp) vs trigonal bipyramidal (tbp)) of the polyhedron surrounding the metal cation is not well-defined; however, a slight preference for the sp description seems indicated, as revealed by the value of the trigonal index[37] τ

(36) Desiraju, G. R.; Steiner T. *The Weak Hydrogen Bond*; Oxford University Press: Oxford, 1999.

(37) Addison, A. W.; Rao, T. N.; Reedijk, J.; Van Rijn, J.; Vershcoor, G. C. *J. Chem. Soc., Dalton Trans.* **1984**, 1349.

Table 2. Bond Lengths (Å) and Angles (deg) Concerning the Coordination Sphere of Compound **8**

Zn(1)−O(1)	1.988(3)
Zn(1)−N(1)	2.108(5)
Zn(1)−N(2)	2.088(5)
Zn(1)−N(3)	2.160(5)
Zn(1)−N(4)	2.198(4)
O(1)−Zn(1)−N(1)	92.2(1)
O(1)−Zn(1)−N(2)	112.6(1)
O(1)−Zn(1)−N(3)	110.6(1)
O(1)−Zn(1)−N(4)	116.8(1)
N(1)−Zn(1)−N(2)	86.6(2)
N(1)−Zn(1)−N(3)	155.7(2)
N(1)−Zn(1)−N(4)	80.5(2)
N(2)−Zn(1)−N(3)	92.1(2)
N(2)−Zn(1)−N(4)	129.2(2)
N(3)−Zn(1)−N(4)	84.5(2)

Scheme 2. $[Zn_2H_{-1}\mathbf{L2}]^{3+}$ Species from Ref 39

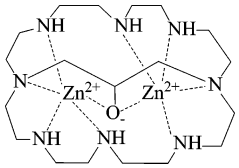

(0.44), given that for ideal sp and tbp geometries τ values of 0 and 1, respectively, are expected. The four nitrogen atoms describing the base of the sp are connected by ethylene chains that show the typical gauche conformation, allowing for the formation of three five-membered chelate rings. The zinc ion is displaced 0.67Å from their mean plane, and is shifted toward the oxygen atom that occupies the apex of the sp. Thus the two coordination polyhedra share the phenolate oxygen atom, and are facing each other. A dihedral angle of 88.4(6)°, which determines a larger bite, defines the conformation of the $N-CH_2-CH_2-N$ moiety that connects the two Zn(II) ions.

Finally, in the crystal lattice, several H-bonds exist between the oxygen atoms of both the perchlorate anions and the hydrogens bound to the secondary amine groups of the ligand.

A search in the Cambridge Structural Database (CSD, version 5.25, November 2003)[38] for analogous dinuclear Zn(II) complexes revealed the structure of a dinuclear Zn(II) alkoxide-bridged octaazacryptate with ligand **L2** (Scheme 2),[39] hereafter called $[Zn_2H_{-1}\mathbf{L2}]^{3+}$. The high level of similarity between the two ligands prompted us to compare the 3D structures of the two cryptates. In the two complexes, the overall coordination environment of the zinc ions is very similar, as qualitatively shown by the superposition of the atoms defining the coordination sphere in the two cryptates, and quantitatively shown by the comparison of the τ indexes (0.47 in $[ZnH_{-1}\mathbf{L2}]^{3+}$). Also, the distance that separates the two cations is similar in the two metal complexes (3.42 Å in $[Zn_2H_{-1}\mathbf{L2}]^{3+}$).

Given this high structural analogy between $[Zn_2(H_{-1}\mathbf{L})]^{3+}$ and $[Zn_2H_{-1}\mathbf{L2}]^{3+}$, and in agreement with the results reported by Kimura et al., we can suppose that **8** could also work in recognizing external species notwithstanding the fact that zinc ions are coordinately almost saturated. This hypothesis was validated by a survey of the crystal data deposited in the CSD concerning dinuclear complexes featuring Zn(II) ions further assembling external species. The retrieved intermetallic Zn−Zn distances in such species compare well with that observed in **8**.

As a final remark, comparison of the overall shapes of $[Zn_2(H_{-1}\mathbf{L})]^{3+}$ and $[H_6\mathbf{L}]^{6+}$ suggests that the skeleton of **L** is very flexible, making the latter a versatile ligand able to model itself to fulfill different geometrical and/or electronic requirements.

Table 3. Logarithm of the Protonation Constants of **L** Determined by Means of Potentiometric Measurements in 0.15 M NMe_4NO_3 (A) or NMe_4Cl (B) Aqueous Solutions as Ionic Medium at 298.1 K

	log K	
reaction	A	B
$\mathbf{L} + H^+ = H\mathbf{L}^+$	10.03(2)[a]	10.20(3)
$H\mathbf{L}^+ + H^+ = H_2\mathbf{L}^{2+}$	9.26(1)	9.24(2)
$H_2\mathbf{L}^{2+} + H^+ = H_3\mathbf{L}^{3+}$	8.67(1)	8.78(1)
$H_3\mathbf{L}^{3+} + H^+ = H_4\mathbf{L}^{4+}$	6.02(1)	6.25(1)
$H_4\mathbf{L}^{4+} + H^+ = H_5\mathbf{L}^{5+}$	2.71(3)	3.69(1)
$H_5\mathbf{L}^{5+} + H^+ = H_6\mathbf{L}^{6+}$		1.96(4)

[a] Values in parentheses are the standard deviations on the last significant figure.

Solution Studies. Basicity. In Table 3, the log K values of the protonation constants of **L** are reported, potentiometrically determined in 0.15 M NMe_4NO_3 aqueous solution at 298.1 K. The neutral species **L** can add up to five acidic protons, forming the $H_5\mathbf{L}^{5+}$ species under the experimental conditions used. Taking into account that the phenol group shows an acidic proton, we could not detect, in this case, the $H_{-1}\mathbf{L}^-$ species that could theoretically be achieved in alkaline solution. Analysis of the protonation constant values starting from the neutral **L** species revealed that it behaves as a rather strong base in the addition of the first three protons, with protonation constant values ranging from 10.03 to 8.67 logarithmic units; a decrease in the fourth protonation step (log $K = 6.02$) and a sharp decrease in the last proton addition (log $K = 2.71$) were observed. This trend suggests an easy availability of the protonation sites up to the $H_3\mathbf{L}^{3+}$ species, in agreement with the topology of the ligands. For these reasons, the three acidic protons in the $H_3\mathbf{L}^{3+}$ species are probably located far from each other on noncontiguous amine groups of the macrocycle. Even though **L** has a the total of eight protonatable sites, the cage topology of the ligand, which assembles many positive charges in a limited space, influences the availability of the amine groups for protonation starting from the addition of the fourth proton, at least under these experimental conditions. This is reflected in a decrease in the protonation constant values in the fourth step that is even more accentuated in the fifth protonation step. The influence of the topology of **L** on basicity is well-highlighted by the comparison of the basicity of **L** with that of the polyazacycloalkane [24]aneN_8, which shows more protonation constants and protonation constant values that are always larger in all the same protonation steps.[40]

Coordination of Metal Ions. The coordination properties of **L** were studied in 0.15 M NMe_4NO_3 aqueous solution at

(38) Allen, F. H. *Acta Crystallogr.* **2002**, *B58*, 380.
(39) Koike, T.; Inoue, M.; Kimura, E.; Shiro, M. *J. Am. Chem. Soc.* **1996**, *118*, 3091.

Table 4. Logarithms of the Equilibrium Constants Determined in 0.15 mol dm^{-3} NMe_4NO_3 at 298.1 K for the Complexation Reactions of **L** with Cu(II) and Zn(II) Ions

reaction	log *K* M = Cu(II)	log *K* M = Zn(II)
$M^{2+} + \mathbf{L} = M\mathbf{L}^{2+}$	22.13(1)[a]	15.55(3)
$M^{2+} + \mathbf{L} + H^+ = MH\mathbf{L}^{3+}$	29.73(1)	23.19(2)
$M^{2+} + \mathbf{L} + 2H^+ = MH_2\mathbf{L}^{4+}$	36.63(2)	29.76(2)
$M^{2+} + \mathbf{L} + 3H^+ = MH_3\mathbf{L}^{5+}$		33.42(2)
$M^{2+} + \mathbf{L} = MH_{-1}\mathbf{L}^+ + H^+$	12.24(2)	4.82(1)
$2M^{2+} + \mathbf{L} = M_2\mathbf{L}^{4+}$	33.76(2)	21.23(1)
$2M^{2+} + \mathbf{L} = M_2H_{-1}\mathbf{L}^{3+} + H^+$	31.11(4)	16.33(1)
$2M^{2+} + \mathbf{L} + H_2O = M_2H_{-1}\mathbf{L}OH^{2+} + 2H^+$	19.88(4)	5.43(2)
$M^{2+} + M\mathbf{L}^{2+} = M_2\mathbf{L}^{4+}$	11.63	5.68
$M^{2+} + MH_{-1}\mathbf{L}^+ = M_2H_{-1}\mathbf{L}^{3+}$	18.87	11.51
$M_2H_{-1}\mathbf{L}^{3+} + OH^- = M_2H_{-1}\mathbf{L}OH^{2+}$	2.50(4)	2.83(3)

[a] Values in parentheses are the standard deviations on the last significant figure.

298.1 K. The stability constants for the equilibrium reactions with Cu(II) and Zn(II) were potentiometrically determined and are reported in Table 4.

L forms both mono- and dinuclear species with the two M(II) ions examined; the dinuclear complexes are the only species existing in solution at pH higher than 6 when the **L**:M(II) molar ratio is 1:2, whereas the mononuclear species are instead prevalent in solution when the L:M(II) molar ratio is 1:1, although dinuclear species are also present at this molar ratio (see Figure 4).

Considering the mononuclear species, some important aspects can be highlighted; **L** forms stable mononuclear complexes, with a log *K* of 22.13 and 15.55 for the addition of Cu(II) and Zn(II) to the neutral species **L**, respectively (see Table 4). These values of the formation reaction are similar to those reported for the same speciation of M(II) with the ligand **L1**.[20b] Taking into consideration that in the case of M(II)/**L1** systems, the coordination environment in the formation of the mononuclear $[M\mathbf{L1}]^{2+}$ species was suggested to be provided by the phenol oxygen together with a triamine subunit, we could suggest a similar coordination arrangement in the same mononuclear species of **L**. However, an involvement of a fourth amine group could also be hypothesized, considering the molecular topology and the crystal structure here reported (Figure 3). The $[M\mathbf{L}]^{2+}$ species undergoes two easy protonations, achieving the $[ZnH_3\mathbf{L}]^{5+}$ and $[CuH_2\mathbf{L}]^{4+}$ species, respectively, confirming that several amine groups are not involved in coordination in the $[M\mathbf{L}]^{2+}$ species.

Moreover, because of the presence of the metal ion, the acidic proton of **L** species can be removed, reaching the anionic form in the $[M(H_{-1}\mathbf{L})]^+$ species. The log *K* value of 18.87 or 11.51 logarithmic units obtained for the addition of the second Cu(II) or Zn(II), with respect to the $[M(H_{-1}\mathbf{L})]^+$ species, indicates the great tendency of **L** to coordinate another M(II) ion, forming stable dinuclear species. The high value of the second metal addition, similar to that of the first addition to the **L** species, leads us to suppose that the two metal ions result in a similar coordination environment, in both mono- and dinuclear species, each stabilized by the amine functions and by the oxygen of the phenolate moiety that bridges the two M(II) ions, probably in the same manner depicted in the crystal structure of Figure 3. The formation constants of the hydroxylated $[M_2(H_{-1}\mathbf{L})OH]^{2+}$ species show lower values than those of the same species of **L1**[20b] (reaction $[M_2(H_{-1}L)]^{3+} + OH^- = [M_2(H_{-1}L)OH]^{2+}$; log $K = 2.50$ and 2.83 for L = **L** vs 7.65 and 5.17 logarithmic units for L = **L1** for Cu(II) and Zn(II), respectively). This weaker tendency to add OH^- can be explained by the lower availability of both metal centers in the $[M_2H_{-1}L]^{3+}$ species of **L** to a guest. This is due to the higher saturation of the binding sites of the metal ions provided by **L** as well as to

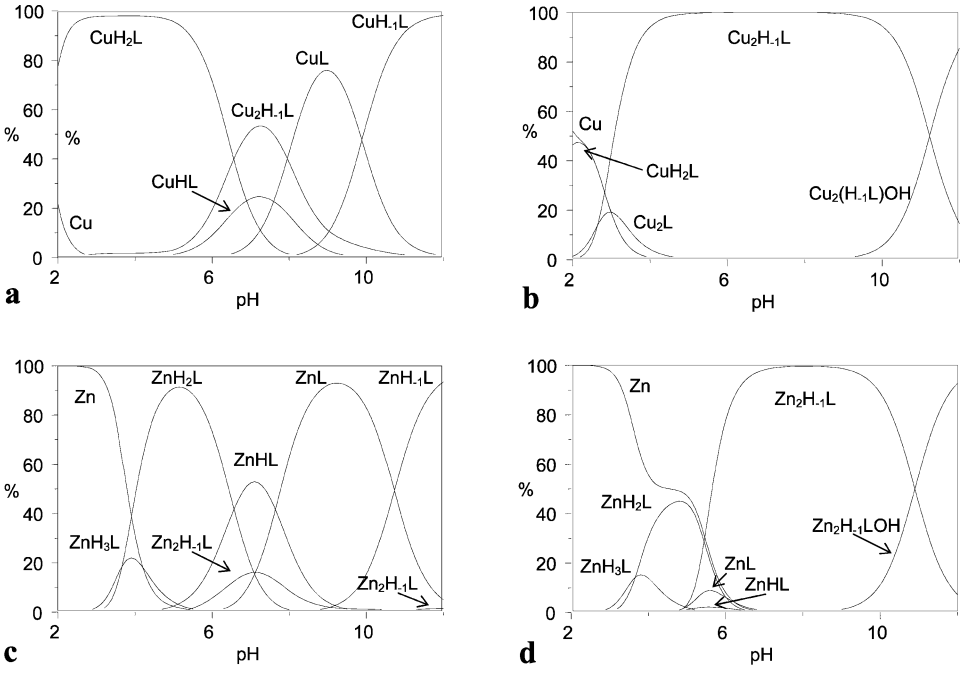

Figure 4. Distribution diagrams of the species for the L/M(II) systems as a function of pH in aqueous solution, $I = 0.15$ mol dm^{-3} NMe_4NO_3, at 298.1 K, [**L**] = 1×10^{-3} mol dm^{-3}: (a) [Cu(II)] = 1×10^{-3} mol dm^{-3}; (b) [Cu(II)] = 2×10^{-3} mol dm^{-3}; (c) [Zn(II)] = 1×10^{-3} mol dm^{-3}; (d) [Zn(II)] = 2×10^{-3} mol dm^{-3}.

the cage topology of **L**, which isolates the metal ions from the medium more than does the topology of **L1**. Both aspects can be seen in Figure 3, which shows the crystal structure of the $[Zn_2(H_{-1}\mathbf{L})]^{3+}$ species in which the donor atoms of **L** fulfill the coordination requirement of the two Zn(II) ions that lodge inside the three-dimensional cavity. In other words, the hydroxylated $[M_2(H_{-1}\mathbf{L})OH]^{2+}$ species are more likely formed by the addition of the OH^- taken from the medium than by the deprotonation of a coordinated water molecule in the $[M_2(H_{-1}\mathbf{L})]^{3+}$ species. The formation of the hydroxylated species, which takes place only at high concentrations of OH^- (see Figure 4b,d), together with the absence of coordinated water molecules in the reported crystal structure supports this hypothesis.

In the dinuclear $[M_2(H_{-1}\mathbf{L1})OH]^{2+}$ species, it was demonstrated that the OH^- bridges the two metals occupying the free fifth-coordination position of both metal ions. In this case, the OH^-, still bridging the two metal ions, should occupy either a sixth or, more probably, a fifth position by removing a coordinated nitrogen atom in a pentacoordination environment of each metal ion, thus decreasing the formation constants of the hydroxylated species.

Analyzing the UV−vis spectra recorded in aqueous solution at pH = 7 and 12, where the $[Cu_2(H_{-1}\mathbf{L})]^{3+}$ and $[Cu_2(H_{-1}\mathbf{L})OH]^{2+}$ species, respectively, are prevalent in solution, we do not observe strong changes in their spectral profiles. This leads us to suppose that the formation of the hydroxylated species does not deeply influence the coordination environment of both Cu(II) ions as well as the phenolic chromophore, thus supporting a pentacoordination of both metal ions in both species. In particular, the spectrum at pH = 7, where the $[Cu_2(H_{-1}\mathbf{L})]^{3+}$ species is prevalent in solution, shows four main bands, st $\lambda_{max} = 239$ (sharp, $\epsilon = 9500$ cm^{-1} mol^{-1} dm^3), 283 (sharp, $\epsilon = 9200$ cm^{-1} mol^{-1} dm^3), 389 (broad, $\epsilon = 350$ cm^{-1} mol^{-1} dm^3), and 583 nm (broad, $\epsilon = 450$ cm^{-1} mol^{-1} dm^3). The two bands at higher energy are due to the n−π* and π−π* transitions of the phenolate group engaged in the coordination of the metals; the other two bands at 389 and 583 nm are ascribed to the phenolate−copper charge transfer and to the d−d* transition band of the metals,[13b] respectively; the spectrum recorded at pH = 12, where $[Cu_2(H_{-1}\mathbf{L})OH]^{2+}$ is prevalent in solution, shows a profile similar to that of the previous one, with a small shift of 4 nm of the d−d* band ($\lambda_{max} = 587$ nm).

In conclusion, the aqueous solution studies underline the capability of **L** to form stable dinuclear species with both M(II) ions examined. The binding properties are similar to those of its precursor **L1**, although the availability of the dinuclear species to act as host for external species seems to be reduced by the cage topology of the ligands and by the presence of a larger number of donor atoms in **L**. However, the presence of the phenolate group, the oxygen of which has the capability to bridge the two metal ions, draws the two metal ions very close to each other (3.33 Å for the zinc complex in the crystal structure), probably with a similar coordination environment.

Binding of Anions. The ability of **L** to act as host for anion guests in aqueous solution was tested for the free ligand as well as for the dinuclear $[Zn_2(H_{-1}\mathbf{L})]^{3+}$ species. Two systems gave interaction and are reported: **(i)** the protonated species of **L** with chloride anion and **(ii)** the dinuclear $[Zn_2(H_{-1}\mathbf{L})]^{3+}$ species with phosphate anion.

(i) The **L**/Cl^- system was studied in aqueous solution by both potentiometric and ^{35}Cl NMR experiments at different pH values. The potentiometric experiments performed in 0.15 M NMe_4NO_3 aqueous solution at 298.1 K in the presence of Cl^- anion (see Experimental Section) showed the formation of the $[H_6\mathbf{L}Cl]^{5+}$ species (log $K = 41.33(3)$ for the $\mathbf{L} + 6H^+ + Cl^- = [H_6\mathbf{L}Cl]^{5+}$ reaction). Because the protonation constant relative to the formation of the $H_6\mathbf{L}^{6+}$ is lacking, it is impossible to calculate the value of the constant for the addition of Cl^- to the protonated species of **L**. However, taking into account that the log $\beta_5 = 36.70$ for the formation of the $H_5\mathbf{L}^{5+}$ species, with the log $K_5 = 2.71$ (see Table 3, column A), we could estimate a log K for the $H_6\mathbf{L}^{6+} + Cl^- = [H_6\mathbf{L}Cl]^{5+}$ reaction between 4.6 and 1.9 logarithmic units. Moreover, the protonation constants, potentiometrically determined in 0.15 M NMe_4Cl aqueous solution at 298.1 K, also showed the formation of the $H_6\mathbf{L}^{6+}$ species, and values for each proton addition were slightly larger in the formation of the $H_4\mathbf{L}^{4+}$ and $H_5\mathbf{L}^{5+}$ species (see Table 3, column B) with respect to those found in 0.15 M NMe_4NO_3 as the ionic medium. This leads us to suppose an interaction of Cl^- anion with these two species that cannot be quantified by potentiometry.

The ^{35}Cl NMR experiments recorded in a D_2O solution helped to detect the interaction between the protonated species of **L** and Cl^-.[41] In fact, ^{35}Cl is a quadrupolar nucleus showing an electric-field gradient that is very sensitive to the symmetric charge distribution around the nucleus. In aqueous solution, the chloride anion has a spherical symmetry, and hence shows a sharp line in the ^{35}Cl NMR spectrum; in contrast, the ^{35}Cl signal of the complexed chloride, lacking the symmetry around it, becomes very broad.[41] The changes in both chemical shift and line-width parameters yielded information on the electronic distribution around the nucleus.

Figure 5 reports the chemical shifts (square block) and the line widths (circles) of the ^{35}Cl signal with respect to the sodium chloride used as an external reference at different pH values, together with the distribution diagram of the species obtained by the potentiometric measurements (lines). The chemical shift varies, from 0.38 ppm in alkaline solution to 12.3 ppm in acidic solution with respect to the free chloride, as does the line width, increasing from 36 to 700 Hz following the same trend of the chemical shift. Figure 5 shows that a variation in both chemical shift and line width is observable with the appearance of the $H_4\mathbf{L}^{4+}$ species, and increases up to the formation of the $H_6\mathbf{L}^{6+}$ species, underlining that the chloride anion interacts with the protonated species of **L** not only in the case of $H_6\mathbf{L}^{6+}$ species but also

(40) Bencini, A.; Bianchi, A.; Micheloni, M.; Paoletti, P.; Garcia-España, E.; Niño, M. A. *J. Chem. Soc., Dalton Trans.* **1991**, 1171.

(41) Hosseini, M. W.; Kintzinger, J. P.; Lehn, J. M.; Zahidi, A. *Helv. Chim. Acta* **1989**, *72*, 1078.

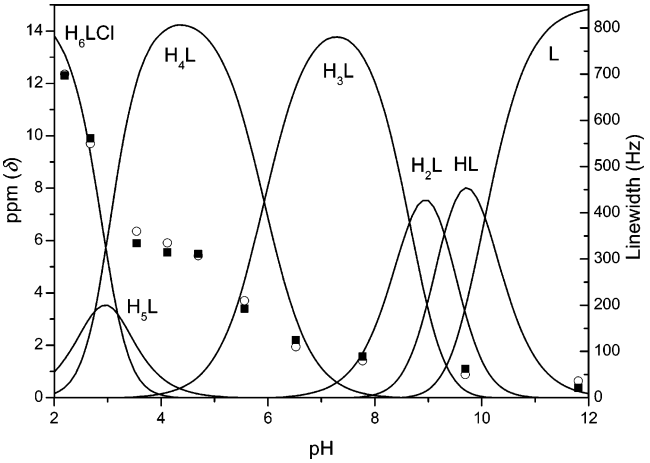

Figure 5. Experimental ^{35}Cl NMR chemical shift (■) and line width (○) of the signal of Cl^- in D_2O solution, together with the distribution diagram of the species for the **L**/Cl^- system (lines) in 0.15 M NMe_4NO_3 aqueous solution, as a function of pH. [**L**] = 1×10^{-2} mol dm^{-3}; [Cl^-] = 5×10^{-2} mol dm^{-3}.

with the other two less-protonated species $H_5\mathbf{L}^{5+}$ and $H_4\mathbf{L}^{4+}$ as suggested above. The large shifts of the ^{35}Cl signal, together with its huge increases in line width, lead us to suppose that one Cl^- is encapsulated inside the cage cavity in a disposition similar to that shown in the crystal structure of Figure 2, even if an exchange, on the NMR time scale, with the external chloride anions can be assumed, because only one ^{35}Cl NMR signal was detected. The change of the macrocyclic conformation and the reduction of the positive charge on the ligand produce the expulsion of the Cl^- from the cavity over pH = 6, as visible in Figure 5. It should also be taken into account that, as shown by UV−vis and ^{1}H and ^{13}C NMR experiments (data not reported), the deprotonation process of $H_4\mathbf{L}^{4+}$ to give $H_3\mathbf{L}^{3+}$ involves the phenolic group present as phenol in $H_4\mathbf{L}^{4+}$ and as phenolate in the $H_3\mathbf{L}^{3+}$ species. In other words, the $H_3\mathbf{L}^{3+}$ species shows a negative charge in a part of the ligand unfavorable to the interaction with an anionic species.

(ii) The $[Zn_2(H_{-1}\mathbf{L})]^{3+}/PO_4^{3-}$ system was studied in a buffered HEPES aqueous solution at pH = 7.0 (see Experimental Section) by UV−vis experiments. To detect the interaction of phosphates (HPO_4^{2-} and $H_2PO_4^-$ are the main species present in solution at this pH value) with the $[Zn_2(H_{-1}\mathbf{L})]^{3+}$ species (the only one existing in solution for the system 2Zn(II)/**L** at this pH value, see Figure 4d), we adopted the competition between phosphate and a further guest used as a sensor. The strategy consists, as already reported in similar cases,[42,43] of using a secondary guest (PCV = pyrocatechol violet in this case) that changes its optical properties when it is bound by the host ($[Zn_2(H_{-1}\mathbf{L})]^{3+}$ in this case). Its affinity for the host is not very high, and thus it can be easily released in the presence of a guest having higher affinity; in this way, the optical response is given by

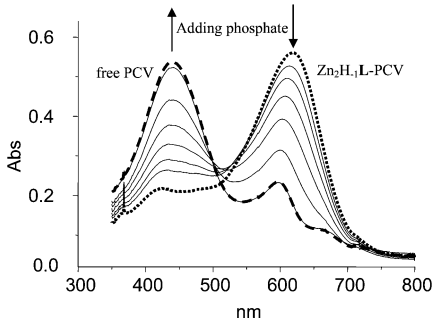

Figure 6. UV−vis spectra of free PCV (- - -) and $[Zn_2H_{-1}\mathbf{L}]^{3+}$ species (···) in an aqueous buffer (HEPES, 1×10^{-2} M) solution at pH = 7.0, [PCV] = 4.0×10^{-5} M, and $[Zn_2H_{-1}\mathbf{L}]^{3+}$ = 4.0×10^{-4} M, and those spectra obtained by adding several amounts of phosphate up to 1 equiv with respect to the $[Zn_2H_{-1}\mathbf{L}]^{3+}$ species (lines).

the free sensor, signaling the coordination of the guest by the host.

PCV is a well-known dye that has strong absorptivity that changes in λ_{max} when it is free or engaged in coordination at pH = 7.[42] In particular, it shows a main band at λ_{max} = 444 nm (ϵ = 13 000 cm^{-1} mol^{-1} dm^3) when it is free or λ_{max} = 624 nm (sharp, ϵ = 14 000 cm^{-1} mol^{-1} dm^3) when it is bound to the metal ions in the host, and the solution appears yellow or blue if PCV is coordinated or not, respectively (see Figure 6).

The dinuclear $[Zn_2(H_{-1}\mathbf{L})]^{3+}$ species is able to bind PCV at pH = 7 as demonstrated by the disappearance of the band at 444 nm (yellow color) and the appearance of the band at 624 nm (blue color; see Figure 6). In this case, a large amount of the $[Zn_2(H_{-1}\mathbf{L})]^{3+}$ species, up to 10 equiv with respect to PCV, must be added to obtain its complete coordination, as confirmed by the invariability of the absorption spectra. This large molar ratio between $[Zn_2(H_{-1}\mathbf{L})]^{3+}$ and PCV denotes that the adduct $[Zn_2(H_{-1}\mathbf{L})]^{3+}$−PCV formed does not have high stability.

When phosphate (using a buffer solution at pH = 7.0) was added to the buffer solution at the same pH value containing $[Zn_2(H_{-1}\mathbf{L})]^{3+}$ and PCV in a 10:1 molar ratio, the turnover of the spectral figure was observed (see lines in Figure 6). This can be explained by the replacement of PCV with phosphate in the adduct; this yields the release of PCV into the medium. In this case, 1 equiv of phosphate with respect to the $[Zn_2(H_{-1}\mathbf{L})]^{3+}$ complex is sufficient to completely release the PCV.

No interaction was observed with the other inorganic anions tested (Cl^-, Br^-, NO_3^-, and SO_4^{2-}) or with the phosphate derivatives 4-nitrophenyl phosphate (NPP) and bis(4-nitrophenyl)phosphate (BNP). This latter observation is in contrast to the results obtained by Kimura and co-workers with the similar ligand **L2**, the $[Zn_2H_{-1}\mathbf{L2}]^{3+}$ species that was able to interact and hydrolyze the NPP^{2-} anion at this pH. In our case, using the same experimental conditions described in ref 39 and monitoring the system by ^{1}H and ^{31}P NMR experiments, we detected no interaction or hydrolysis product (i.e., phosphate and 4-nitrophenol) after maintaining the system at 50 °C for a week.

These data could be interpreted by taking into account that although similar, the two ligands **L** and **L2** are not the same

(42) Han, M. S.; Kim, D. H. *Angew. Chem.* **2002**, *41*, 3809.
(43) (a) Fabbrizzi, L.; Marcotte, N.; Stomeo, F.; Taglietti, A. *Angew. Chem.* **2002**, *41*, 3811. (b) Hortala, M. A.; Fabbrizzi, L.; Marcotte, N.; Stomeo, F.; Taglietti, A. *J. Am. Chem. Soc.* **2003**, *125*, 20. (c) Han, M. S.; Kim, D. H. *Bioorg. Med. Chem. Lett.* **2003**, *13*, 1079.

molecule. The main differences are (i) the bridging chain between the two nitrogen atoms of the [24]aneN_8 system in **L** is longer than that in **L2** (two more carbon atoms than in **L2**) and (ii) the donor capability of the oxygen atom in **L** is greater than that in **L2**. This could make the dinuclear Zn(II) core less accessible to the NPP anion in the complex species of **L** with respect to **L2**.

Conclusion

The newly synthesized and characterized ligand **L** can be described as being derived from the [24]aneN_8 moiety, in which two opposite nitrogen atoms are bridged by a chain containing a phenolic function; it can also be compared to ligand **L1**, in which the four primary amine groups are connected in a 1+2 cyclization scheme with the suitable fragment. All the same, **L** is a cage with a large macrobicyclic cavity. Analysis of the basicity of **L** in aqueous solution showed a lower number of protonated species than in the [24]aneN_8 monocyclic precursor even though it has the same number of protonatable sites; this is attributed to the cage topology of **L**, which concentrates the positive charge of the ammonium group in a limited space, obstructing a degree of protonation greater than that in $H_5\mathbf{L}^{5+}$. However, this aspect allows **L** to bind anions that can fit the cavity and are able to form H-bonds. A study of interactions of **L** with the chloride anion showed that highly protonated species of it (i.e., the $H_4\mathbf{L}^{4+}$, $H_5\mathbf{L}^{5+}$, and mainly $H_6\mathbf{L}^{6+}$ species) are able to bind one chloride ion. The anion is probably coordinated in solution by the ammonium groups of **L** inside the cavity with which it interacts both by electrostatic forces and via H-bond. In fact, one of these species ($H_6\mathbf{L}^{6+}$) was isolated and characterized by X-ray crystallography, and shows one of the six chloride counterions lodged inside the cavity of **L**, much like a ball in a baseball glove, stabilized with a thick H-bond network with several ammonium groups.

L is able to form dinuclear complexed species with Cu(II) and Zn(II) transition-metal ions. The phenol moiety, as phenolate, plays its coordinating role in these species by bridging the two metal ions and drawing them inside the macrobicyclic cavity, coordinated by all amine groups of the ligand. The two metals were found to be quite isolated by the medium, as revealed by the crystal structure of the dinuclear $[Zn_2H_{-1}\mathbf{L}]^{3+}$ species. However, this species still maintains the property of host to a guest as **L1**; in this case, the detected guests were the hydroxide and the phosphate anions. In particular, studies of competition with pyrochatecol violet and phosphate guests highlighted that the $[Zn_2H_{-1}\mathbf{L}]^{3+}$ species is able to bind a phosphate anion at physiological pH.

In conclusion, the preliminary studies of anion binding have demonstrated the capability of both protonated and complexed dinuclear species of **L** to bind simple inorganic anions in solution. Therefore, it would be of interest to extend the binding properties of **L** to other anions of biological relevance, such as carboxylate or others containing phosphate groups such as ATP, ADP, or the series of glucose phosphates that can be bound by the dinuclear species of **L** as well as by the protonated species of it.

Acknowledgment. The authors thank CRIST (Centro Interdipartimentale di Cristallografia Strutturale, University of Florence), where the X-ray measurements were carried out, and Marche Regional Council, CIPE2002 Project, for financial support.

Supporting Information Available: Listings of tables of crystallographic data, positional parameters, isotropic and anisotropic thermal factors, and bond distances and angles in CIF format. This material is available free of charge via the Internet at http://pubs.acs.org.

IC051304V